

A SIMPLE DYNAMICAL MODEL FOR STARS IN THE GALACTIC HALO

HERWIG DEJONGHE AND TIM DE ZEEUW
 The Institute for Advanced Study

Received 1987 September 30; accepted 1987 December 4

ABSTRACT

The Bahcall-Schmidt-Soneira Galaxy potential can be fitted accurately by a Stäckel potential. This provides an effective third integral that can be used in the interpretation of the kinematics of various galactic populations. As an example we use Stäckel dynamics to analyze the observed kinematics of K giants in the Galactic halo. We assume that the stars are distributed on thin tube orbits (shell orbits). This is the Stäckel generalization of the circular orbit model in a spherical potential. We find that the observed line-of-sight velocity dispersion is reproduced for Galactic altitudes larger than 10 kpc. Application of the Stäckel formalism to the kinematics of other galactic populations should be rewarding.

Subject headings: galaxies: The Galaxy — stars: stellar dynamics

I. INTRODUCTION

Various samples of halo stars exist with observed radial velocities (Pier 1982, 1983; Ratnatunga and Freeman 1985; Sommer-Larsen and Christensen 1986; Norris 1986; Sandage 1987). The line-of-sight velocity dispersions are surprisingly small for stars at high altitudes ($|z| > 10$ kpc). They are about half the radial dispersion of the stars in the solar neighborhood and also much smaller than expected on basis of a reasonable assumption for the value of the *in situ* circular velocity (cf. Freeman 1987).

White (1985) addressed this problem and showed that the small velocity dispersions can be understood in a natural way by assuming that the stars at high altitudes are distributed predominantly on nearly circular orbits, i.e., on orbits with small radial excursions. He arrived at this conclusion by using a spherical potential for the Galactic halo. This enabled him to specify mathematically convenient density components in dynamical equilibrium by choosing simple distribution functions. He then reproduced the observed velocity dispersions by a superposition of flattened components. White pointed out that more detailed models can be obtained by using non-spherical potentials.

A first attempt in this direction was made by Levison and Richstone (1986). These authors used a scale-free model with a flat rotation curve (i.e., a logarithmic potential) and were able to construct components by superposition of individual stellar orbits via linear programming, subject to the constraint that the observed dispersions should be reproduced. They confirmed White's result that the important orbits are the ones that have relatively small radial thickness.

Recently, Sommer-Larsen (1987) reproduced the same data with a simple two-component model in a spherical potential. It consists of a Michie-Bodenheimer-type component (Richstone and Tremaine 1984) and a component entirely made of stars in circular orbits. Thus, unlike White and Levison and Richstone, he was able to fit the data with spherical components only.

The above studies reproduce the observed kinematics of the halo stars by models with an anisotropic velocity distribution and in effect assume that the distribution function of these stars depends on three integrals of motion. A spherical potential admits four isolating integrals. In addition to the energy E , the three components L_x , L_y , and L_z of the angular momentum vector L are conserved as well. For simplicity, anisotropic

spherical models often are constructed by use of a distribution function $F = F(E, L^2)$. If there is a preferred axis of rotation, it is natural to assume that F depends on L_z also. This is the approach adopted by White (1985) and by Sommer-Larsen (1987). It has the advantage that the density components can be specified in analytic form.

For axisymmetric models generally two integrals exist, the energy E and the component of the angular momentum parallel to the symmetry axis, L_z , say. Numerical orbit calculations have shown that in realistic Galactic potentials most stars have an effective third integral. No general expression exists for this extra integral. For this reason Levison and Richstone (1986) constructed components by numerical superposition of individual stellar orbits. Since the orbits indeed are constrained by a third integral, the resulting distribution function depends on it as well, although this integral is not known explicitly. The scale-free axisymmetric models employed by Levison and Richstone have the advantage that their mathematical description is essentially one-dimensional.

It is natural to ask whether we can use White's and Sommer-Larsen's analytic approach, but in an axisymmetric potential. This requires a set of axisymmetric potentials for which the third integral is exact. Such potentials were discovered by Stäckel in 1890, and have been applied in galactic dynamics by a number of authors (Kuzmin 1956; Hori 1962; van de Hulst 1962). In this paper, we use these Stäckel potentials as a basis for a simple dynamical description of the Population II stars in our Galaxy.

In § II we review the essentials of dynamics in axisymmetric Stäckel models. In § III we produce a Stäckel potential that fits the Bahcall-Schmidt-Soneira Galaxy model (Bahcall and Soneira 1980; Bahcall, Schmidt, and Soneira 1982) globally. As an example of the use of this fit, we consider in § IV the kinematics of shell orbits—which are the generalizations of the circular orbits in a spherical model—and compare them with the observations. Implications of our results are discussed briefly in § V. The reader who is not interested in the theoretical details should concentrate on §§ IIa–IIc and then skip to § IV.

II. AXISYMMETRIC SEPARABLE DYNAMICS

An axisymmetric Stäckel potential admits an exact third integral of motion because the Hamilton-Jacobi equation

separates in prolate spheroidal coordinates. We first describe these coordinates, and then turn to the equations of motion and the resulting stellar orbits. For a detailed discussion see Kuzmin (1956), Hori (1962), and de Zeeuw (1985, hereafter Paper I).

a) Geometry

Define spheroidal coordinates as the triple (λ, ϕ, v) , where ϕ is the azimuthal angle in ordinary cylindrical coordinates $[\varpi = (x^2 + y^2)^{1/2}, \phi, z]$, and λ and v are the two roots for τ of

$$\frac{\varpi^2}{\tau + \alpha} + \frac{z^2}{\tau + \gamma} = 1, \quad (1)$$

where α and γ are constants, and $-\gamma \leq v \leq -\alpha \leq \lambda$. The coordinate surfaces are confocal spheroids ($\lambda = \lambda_0$) and hyperboloids of revolution ($v = v_0$) with the z -axis as rotation axis. The spheroids are prolate, and the hyperboloids have two sheets. λ and v are elliptic coordinates in each meridional plane $\phi = \phi_0$, with foci on the z -axis at $z = \pm \Delta = \pm(\gamma - \alpha)^{1/2}$. A point (λ, v) generally corresponds to two points $(\varpi, \pm z)$ in the meridional plane (see Fig. 1 below). Further properties of prolate spheroidal coordinates can be found in, e.g., Morse and Feshbach (1953).

A choice of the focal distance determines the spheroidal coordinate system completely. The values of α and γ are then determined up to an additive constant. When $\alpha = \gamma$, the spheroids become spheres, and the hyperboloids all degenerate to their asymptotic cones. In that case equation (1) has only one root $\lambda = r^2 - \alpha$, with $r^2 = x^2 + y^2 + z^2$.

b) Equations of Motion

A gravitational potential V_s is of Stäckel form in the coordinates (λ, ϕ, v) , if it can be written as

$$V_s = -\frac{f(\lambda) - f(v)}{\lambda - v}, \quad (2)$$

where $f(\tau)$ is an arbitrary function ($\tau = \lambda, v$). The special form (2) causes the Hamilton-Jacobi equation to separate (Paper I, § IV). This has as a consequence that three of the six equations of motion can be integrated, yielding three constants of the motion $E, I_2,$ and I_3 . The constant E is the energy per unit mass of a star, and $I_2 = \frac{1}{2}L_z^2$. I_3 is the famous third integral of galactic dynamics (cf. Oort 1965). Near the Galactic plane it reduces to the energy in the z -motion, and at large radii, where the potential is nearly spherical, it is approximately equal to $\frac{1}{2}(L^2 - L_z^2)$.

The remaining equations of motion are three first-order differential equations. They can be written as

$$\begin{aligned} v_\tau^2 &= \frac{1}{4} \frac{\tau - \sigma}{(\tau + \alpha)(\tau + \gamma)} \dot{\tau}^2 \\ &= 2 \frac{\tau + \gamma}{\tau - \sigma} \left[E - \frac{I_2}{\tau + \alpha} + \frac{f(\tau) - I_3}{\tau + \gamma} \right], \end{aligned} \quad (3a)$$

where $(\tau, \sigma) = (\lambda, v)$ or vice versa, and

$$v_\phi^2 = (\varpi \dot{\phi})^2 = \frac{2}{\varpi^2} I_2 = \frac{L_z^2}{\varpi^2}. \quad (3b)$$

The velocities $v_\lambda, v_\phi,$ and v_v are the components of the velocity vector in the local Cartesian coordinate system.

c) Orbits

The general orbits in an oblate axisymmetric Stäckel potential are all short axis tubes¹ (Hori 1962; Paper I, § VIb). In the meridional plane such an orbit fills the area defined by (Fig. 1)

$$-\gamma \leq v \leq v_0, \quad \lambda_1 \leq \lambda \leq \lambda_2, \quad (4)$$

where v_0, λ_1 and λ_2 are the turning points of the orbit, defined as the values of v and λ for which $v_v = 0$ and $v_\lambda = 0$, respectively. It is possible to express quite generally the integrals of motion $H, I_2,$ and I_3 , as functions of the turning points (cf. de Zeeuw 1988, hereafter Paper II). We can therefore equally well use the turning points as the integrals of the motion. As is evident from Figure 1, the turning points offer intuitive insight into the dynamics.

A short axis tube orbit has a definite sense of rotation around the z -axis, and librates in λ and v . The periods $T_\lambda, T_\phi,$ and T_v of the $\lambda, \phi,$ and v oscillations can be calculated relatively easily, due to the separation of the Hamilton-Jacobi equation. They are discussed *in extenso* in § VIII of Paper I.

In this paper we concentrate on the special short axis tubes that have no thickness in the λ coordinate, so that $\lambda_1 = \lambda_2$. We will refer to these infinitesimally thin short axis tubes as *shell orbits* (Bishop 1987; Paper II). Motion in a shell orbit can be regarded as motion in an elliptic orbit in a plane whose normal is precessing around the z -axis on a cone with fixed top angle (see Fig. 2). The precession period T_p is given by

$$\frac{1}{T_p} = \frac{1}{T_v} - \frac{1}{T_\psi}, \quad (5)$$

where ψ denotes the position angle in the orbital plane, and T_ψ is the period in ψ . In this definition, the precession period is positive if the plane of the orbit precesses in the sense opposite to that of the orbital motion. It is easily seen that such an orbit will eventually cover the whole shell area, unless there happens to be a resonance between the rotation and precession rates. It follows that a perturbation (in the star density, for example), when applied at some particular time, will not remain confined to the plane of the orbit, but will eventually be found with finite probability over the whole shell area due to the precession of the plane of the orbit. This spreading will occur on a time scale that is of the order of the precession time T_p . In the spherical limit there is a 1:1 resonance between the rotation and precession periods, so that every shell orbit breaks up in a continuum of circular orbits.

We emphasize that Stäckel potentials, though clearly special, offer important bonuses which compensate for the restrictions on the mathematical form of the potential:

1. Every orbit has three explicit integrals of motion. Numerical orbit calculations in more realistic galaxy potentials show that only a small fraction of the stars are on stochastic trajectories, and that nearly all orbits are short axis tubes (Ollongren 1962; Martinet and Mayer, 1975).

2. Stäckel potentials can have arbitrary flattening and describe models with a large variety of radial density profiles (de Zeeuw, Peletier, and Franx 1986). Any spherical potential can be obtained as a limiting case of equation (2).

3. It is possible to calculate density components in a Stäckel potential in analytic form, by assumption of specific forms

¹ In the original nomenclature due to Ollongren (1962), an orbit of this kind was referred to as a box orbit. That name is now reserved for one of the four main orbit families in a triaxial galaxy (Schwarzschild 1979).

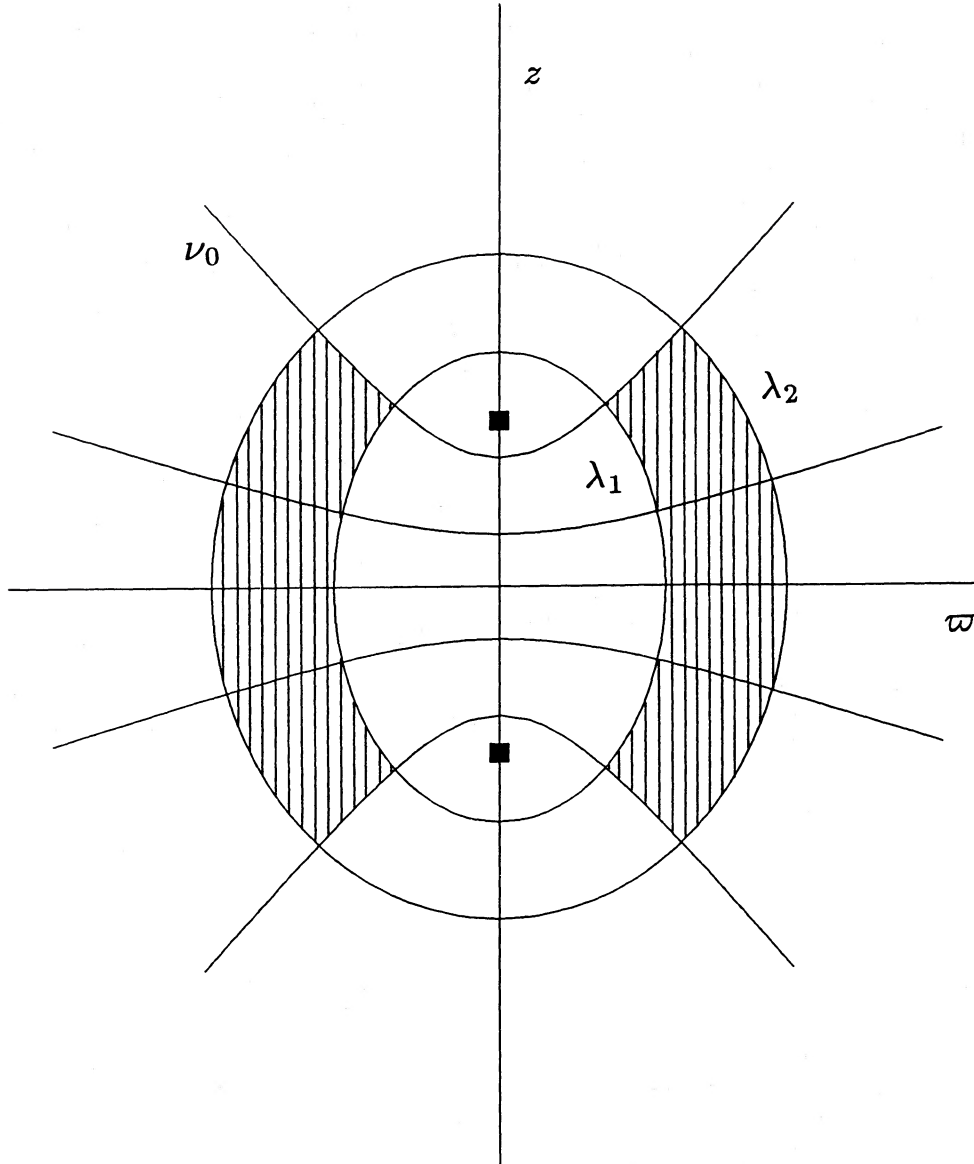


FIG. 1.—The region in the meridional plane occupied by a short axis tube orbit (shaded area). The black squares indicate the position of the foci of the spheroidal coordinates.

$F(E, I_2, I_3)$ for the distribution function, just as was done by White (1985) for the spherical case (Dejonghe and de Zeeuw 1988, hereafter DZ).

d) Kinematical Properties

The velocity ellipsoids for equilibrium components in Stäckel potentials are everywhere aligned with the spheroidal coordinate system (λ, ϕ, ν) (Eddington 1915). The values of the dispersions $\sigma_\lambda, \sigma_\phi,$ and σ_ν in the velocities $v_\lambda, v_\phi,$ and v_ν can be calculated by taking moments of the distribution function, or by direct solution of the equations of stellar hydrodynamics (see DZ). However, in general a given mass density does not uniquely specify a distribution function that depends on three integrals. Hence the equations of stellar hydrodynamics have no unique solution for σ_λ and $\sigma_\nu,$ given ρ and V_S .

From the studies of White (1985), Levison and Richstone (1986), and Sommer-Larsen (1987), we know that the components required for the description of the halo stars of interest

must correspond to superpositions of short axis tubes with a rather small radial epicyclic motion. For this reason we consider the case of the infinitesimally thin short axis tubes, i.e., the shell orbits. In this case the stellar hydrodynamical equations have a unique solution (see Paper II):

$$\rho \sigma_\nu^2 = \frac{1}{|\nu + \alpha|} \int_\nu^{-\alpha} (\lambda - \sigma) \rho(\lambda, \sigma) R(\sigma, \sigma, \lambda, \lambda) d\sigma,$$

$$\langle v_\phi^2 \rangle = 2(\lambda + \alpha) R(\nu, -\alpha, \lambda, \lambda) - \frac{\lambda + \alpha}{\lambda - \nu} \sigma_\nu^2. \quad (6)$$

Here $R(\tau_1, \tau_2, \tau_3, \tau_4)$ is the negative of the third-order divided difference of $(\tau + \alpha)f(\tau)$, with $f(\tau)$ defined in equation (2), i.e.,

$$R(\tau_1, \tau_2, \tau_3, \tau_4) = \sum_{\substack{i=1 \\ 1 \leq j, k, l \leq 4 \\ i \neq j \neq k \neq l}}^4 \frac{(\tau + \alpha)f(\tau)}{(\tau_i - \tau_j)(\tau_i - \tau_k)(\tau_i - \tau_l)}. \quad (7)$$

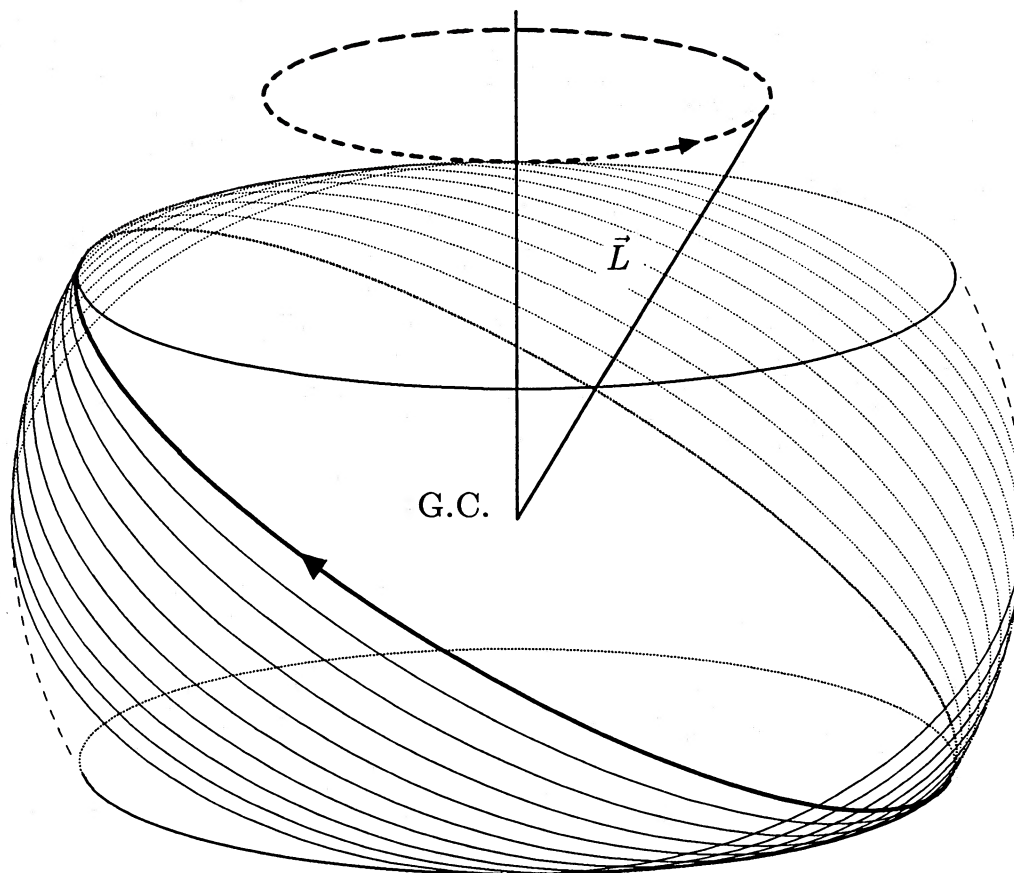


FIG. 2.—Shell orbits as precessing ellipses. The Galactic center and the direction of the Galactic pole are indicated.

Properties and special values of the R -function are discussed in Paper II.

The distribution function for a density built of shell orbits only can be written as a one-dimensional quadrature. It is positive, and hence physical, for homogeneous or centrally concentrated densities (Bishop 1987; Paper II). Since our density components will have this property, there is no immediate need to calculate shell orbit distribution functions explicitly, especially since equation (6) gives the dispersions directly.

The expression for the maximum mean streaming is obtained by calculating the mean of v_ϕ over the distribution function associated with the given ρ (Paper II), assuming that all stars rotate in the same sense:

$$\rho \langle v_\phi \rangle = \frac{2}{\pi} \frac{[2(\lambda + \alpha)R(v, -\alpha, \lambda, \lambda)]^{1/2}}{\lambda - v} \left\{ (\lambda + \alpha)\rho(\lambda, -\alpha) - \int_v^{-\alpha} E(k) \frac{\partial}{\partial \sigma} [(\lambda - \sigma)\rho(\lambda, \sigma)] d\sigma \right\}, \quad (8)$$

where $E(k)$ is the complete elliptic integral of the second kind with modulus

$$k^2 = \frac{(v - \sigma)R(v, \sigma, \lambda, \lambda)}{(v + \alpha)R(v, -\alpha, \lambda, \lambda)}. \quad (9)$$

Thus, for a given density in an oblate axisymmetric Stäckel potential, the kinematical properties of the shell orbit model can be calculated by simple one-dimensional calculations.

We note that $\langle v_\phi \rangle$ as given in equation (8) is distinct from the circular velocity in the equatorial plane, i.e., the rotation curve. The circular orbits in the equatorial plane have turning points $v_0 = -\gamma$ and $\lambda_1 = \lambda_2 = \lambda_0$. By use of the equations of motion it follows that the circular velocity $v_c(\varpi)$ is given by

$$v_c^2(\varpi) = 2(\lambda_0 + \alpha)R(-\gamma, -\alpha, \lambda_0, \lambda_0) = \frac{2(\lambda_0 + \alpha)[f(\lambda_0) - f(-\gamma) - (\lambda_0 + \gamma)f'(\lambda_0)]}{(\lambda_0 + \gamma)^2},$$

$$\lambda_0 + \alpha = \varpi^2. \quad (10)$$

III. GLOBAL FIT

In order to apply the preceding formalism to the dynamics of the Galaxy, we need to approximate the Galactic potential by a Stäckel potential. Since we deal with the determination of kinematical quantities for a component in dynamical equilibrium in a given potential, we need to consider, explicitly or implicitly, the distribution function $F(E, I_2, I_3)$ for that component. Since none of the three integrals contains derivatives of the potential, the error in any kinematical quantity due to inaccurate fitting, or limited knowledge of the potential, will be of the order of the error in the fit to the potential. Any quantity that contains derivatives of the potential, such as the rotation curve, can be subject to large errors (see § IIIb).

We remark that, if we were to determine the evolution of a (nonequilibrium) configuration in the same potential, it follows from the collisionless Boltzmann equation that the deviations

in the partial derivatives of the potential (i.e., the forces) are the dominant sources of the errors, which, again, could be substantial.

a) Method

Consider a potential $V(\varpi, z)$. We wish to approximate V by a Stäckel potential V_S of the form (2). Thus, we need to determine a prolate spheroidal coordinate system (λ, ϕ, ν) and the functions $f(\lambda)$ and $f(\nu)$ in such a way that expression (2) fits V globally as close as possible. It is clear that a procedure for doing this should involve some sort of averaging, and should give the correct answer if V happens to be exactly of Stäckel form. De Zeeuw and Lynden-Bell (1985) describe such a method for triaxial Stäckel models. Their procedure simplifies considerably in the oblate limit (see also de Zeeuw 1984).

First pick a prolate spheroidal coordinate system (λ, ϕ, ν) by choosing the value of $\Delta = (\gamma - \alpha)^{1/2}$ (see § IIa). Transform the given potential $V(\varpi, z)$ to $V(\lambda, \nu)$ by use of the relations

$$\varpi^2 = \frac{(\lambda + \alpha)(\nu + \alpha)}{\alpha - \gamma}, \quad z^2 = \frac{(\lambda + \gamma)(\nu + \gamma)}{\gamma - \alpha}. \quad (11)$$

Then calculate the auxiliary function $\chi(\lambda, \nu)$ by

$$\chi(\lambda, \nu) = -(\lambda - \nu)V(\lambda, \nu). \quad (12)$$

If V happens to be of Stäckel form in the chosen coordinates, then $\chi(\lambda, \nu) = f(\lambda) - f(\nu)$. In that case we can find $f(\lambda)$ and $f(\nu)$ by averaging χ over ν and over λ , respectively. In the more general case we do exactly the same, and we define the averages

$$\begin{aligned} \langle \chi, \lambda \rangle &= \frac{1}{N} \int_{\nu_-}^{\nu_+} \chi(\lambda, \nu) N(\nu) d\nu, \\ \langle \chi, \nu \rangle &= \frac{1}{\Lambda} \int_{\lambda_-}^{\lambda_+} \chi(\lambda, \nu) \Lambda(\lambda) d\lambda, \\ \bar{\chi} &= \frac{1}{\Lambda N} \int_{\nu_-}^{\nu_+} \int_{\lambda_-}^{\lambda_+} \chi(\lambda, \nu) \Lambda(\lambda) N(\nu) d\lambda d\nu, \end{aligned} \quad (13)$$

where $\Lambda(\lambda)$ and $N(\nu)$ are weighting functions that have to be chosen such that the integrals

$$\Lambda = \int_{\lambda_-}^{\lambda_+} \Lambda(\lambda) d\lambda, \quad N = \int_{\nu_-}^{\nu_+} N(\nu) d\nu, \quad (14)$$

are finite. The values of ν_- , ν_+ , λ_- , and λ_+ determine the area in the meridional plane in which the potential V is fitted. A global fit is obtained by choosing $\nu_- = -\gamma$, $\nu_+ = \lambda_- = -\alpha$ and $\lambda_+ = \infty$.

With these definitions, we calculate $f(\lambda)$ and $f(\nu)$ from

$$f(\lambda) = \langle \chi, \lambda \rangle - \frac{1}{2} \bar{\chi}, \quad f(\nu) = \frac{1}{2} \bar{\chi} - \langle \chi, \nu \rangle. \quad (15)$$

This gives the functions $f(\lambda)$ and $f(\nu)$ that define a Stäckel potential V_S that fits V in an average sense in the chosen prolate spheroidal coordinates (λ, ϕ, ν) . In order to improve the fit, one may repeat this process for different coordinate systems, i.e., for different values of $\gamma - \alpha$. We note that the constant $\frac{1}{2} \bar{\chi}$ has been included to ensure that $f(\lambda) = f(\nu)$ at the foci, where $\lambda = \nu = -\alpha$, so that V_S is well-defined there.

If V happens to be of Stäckel form in the chosen coordinates, then equation (15) gives the desired result. If V equals V_S in some other prolate spheroidal coordinate system, then, by repetition of the procedure, one will eventually find a coordinate system in which the fit is exact. The choice of the weighting functions $\Lambda(\lambda)$ and $N(\nu)$ is unimportant if $V = V_S$. For the

general case, the weighting functions may be chosen to put emphasis on the fitting where it is most important for the problem at hand. A good guess for the position of the foci can be made in a number of ways. These are discussed by de Zeeuw and Lynden-Bell (1985).

We note that by decreasing the ν -extent of the region of fitting, it is possible to obtain a fit to the given potential close to the equatorial plane that is arbitrarily accurate. Fitting of a Stäckel potential in the neighborhood of a single point can be done by the above technique also. A more direct method is described by van de Hulst (1962) (see also de Zeeuw 1984).

Finally, the above equations follow from the variational principle that minimizes $(\chi - \chi_S)^2$, and in that sense gives the best overall fit. This means, however, that $(V - V_S)^2$ is weighted with $(\lambda - \mu)^2 \Lambda(\lambda) N(\nu)$, which vanishes at the foci. This low weight close to the foci can lead to a poor fit there, so it may be necessary to modify the weighting functions near the foci in order to ensure a smooth potential.

b) Application to a Galaxy Model

The prescriptions of the previous paragraph are relatively easy to implement numerically, once one decides upon the following:

1. *A potential.*—We choose the Bahcall-Schmidt-Soneira (1982) potential, in an implementation by D. Gilden. For comparison we also consider the Caldwell-Ostriker (1981) potential. Both versions of the Galactic potential were kindly made available to us by L. Aguilar.

2. *Weight functions.*—We take the following rational functions for $N(\nu)$ and $\Lambda(\lambda)$:

$$\begin{aligned} N(\nu) &= \frac{(v + \gamma)^{c_\nu} |v + \alpha|^d}{(\gamma - \alpha)^{c_\nu}}, \\ \Lambda(\lambda) &= \frac{(b - \alpha)^{c_\lambda} (\lambda + \alpha)^d}{(\lambda + b)^{c_\lambda}}, \end{aligned} \quad (16)$$

where b , d , c_λ , and c_ν are parameters. The resulting integrals (14) are convergent as long as $c_\lambda > d + 1 > 0$, $b > \alpha$, and $c_\nu > -1$. These parameters should be chosen according to the region of interest. A negative value of c_ν , or d , assigns more weight to the disk or the foci, respectively. Also, adding weight to the disk worsens the fit around the foci. The parameters b and c_λ are included in expressions (16) for the sake of generality. Their precise values, if within the above bounds, are relatively unimportant. We adopt $b = 0$ and $c_\lambda = 5$.

3. *Region of fit.*—This is the region in the (ϖ, z) plane where the goodness of fit is judged. We have performed fits for two regions, the first one for the whole meridional plane out to about 30 kpc ("global" fit). The second one is in a region limited by two ellipses of constant λ and a hyperbola of constant ν , roughly embedded in a rectangle with $3 \leq \varpi \leq 30$ kpc and $|z| \leq 60$ kpc ("local" fit).

The fitting procedure has been set up so as to find the best fitting Δ , which defines the prolate spheroidal coordinate system (see § IIa), for given weight function parameters. The goodness of fit depends only marginally on the particular weight function, at least for reasonable choices of the parameters c_ν and d (i.e., not too far from zero and according to the region of interest). Of course, Δ does depend on these parameters, since they determine the distribution of weights in the (ϖ, z) -plane. The goodness of fit (minimax) has been calculated in each of the two regions mentioned above. The (absolute)

errors were normalized with the dynamic range of the potential in the fitting region.

For the global fit we use $c_v = d = 0$, and we find a best value of Δ equal to 0.88 kpc. The error in the fit nowhere exceeds $\pm 3\%$, with the largest deviation occurring in the center, and a typical value of 1.5%. The local fit has $c_v = -0.5$ and $d = 0$. We find a value of Δ equal to 0.93 kpc, and an error of $\pm 2\%$ over the whole region.

The function $f(\tau)$ is obtained numerically, but is monotonically increasing and smooth enough to be approximated by a simple interpolating function. We write

$$\ln f(\tau) = \sum_{i=0}^k A_i \tau^i, \quad (17)$$

with

$$t = \frac{2 \ln \tau - \ln \lambda_m - \ln(-\gamma)}{\ln \lambda_m - \ln(-\gamma)}, \quad (18)$$

and A_i and λ_m constants. For fixed Δ we are still free to choose the value of γ . We use this freedom to adopt a value of γ for which the function $\ln f(\tau)$ becomes approximately linear. We take $\gamma = -10^{-6}$ and $k = 11$ and list the values of the constants A_i and λ_m for the global fit in Table 1.

In Figure 3 we compare the rotation curve calculated for the global fit, as given by equation (10), with that obtained from the exact Bahcall-Schmidt-Soneira potential. The typical differences are well within the observational errors. We conclude that the global Stäckel fit is excellent, better even than we would have expected from the good fit to the potential itself. This good representation of the Galactic rotation curve is especially gratifying, since our procedure does not fit any derivatives of the potential. We expect that the corresponding density distribution, which depends on the second derivative of $f(\tau)$, may differ considerably from the actual density distribution of the Galaxy, especially in the central regions.

TABLE 1
COEFFICIENTS IN REPRESENTATION OF $f(\tau)$

Coefficient	Global Fit
λ_m	901.7700
A_0	9.866244
A_1	8.850006
A_2	-4.267299
A_3	-3.921225
A_4	11.48199
A_5	24.24413
A_6	-19.05341
A_7	-50.02188
A_8	14.83199
A_9	44.59103
A_{10}	-4.135184
A_{11}	-15.03169

It should be noted that one can use equation (10) to determine $f(\lambda)$ directly from the observed rotation curve, for each choice of α and γ . This is equivalent to fitting in the equatorial plane only (cf. § IIIa), and additional information is needed to specify $f(v)$. Early examples of an approach along these lines were given by Wayman (1959) and Hori (1962), both of whom fitted a Stäckel potential to the Schmidt (1956) model of the Galaxy.

For the Caldwell and Ostriker (1981) potential, we find a different function $f(\tau)$, but very similar values for Δ with errors of the same magnitude. In what follows we shall therefore consider only the Bahcall-Schmidt-Soneira potential.

IV. A SIMPLE MODEL

We now employ the Stäckel fit to describe the kinematics of the Population II K giants at high Galactic altitude. Our analysis is intended as an illustration of the use of Stäckel dynamics, and we restrict ourselves to data obtained by Ratna-

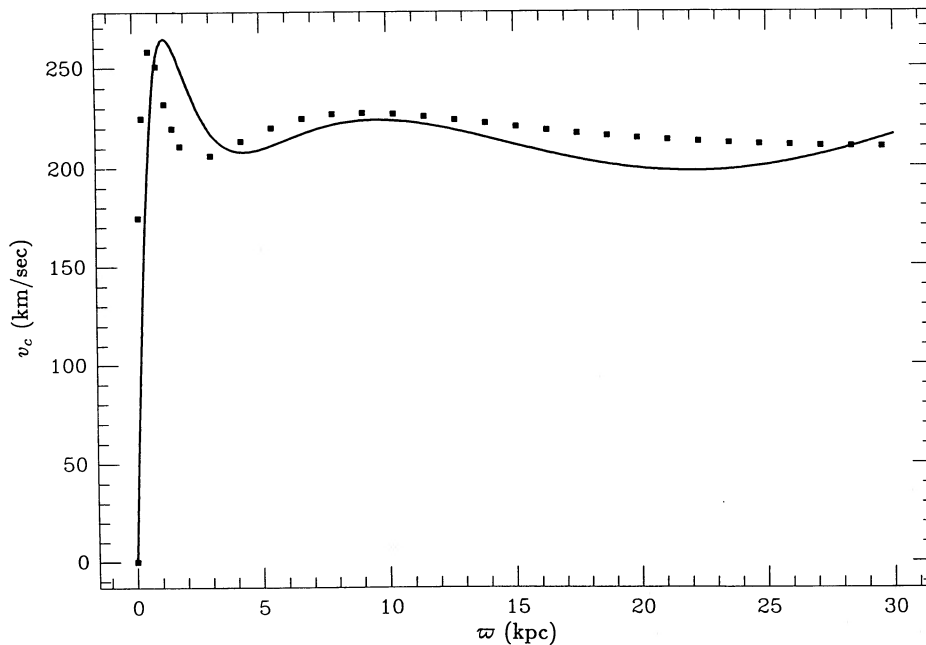


FIG. 3.—Rotation curve corresponding to the global fit described in the text. The black squares are the rotational velocities given by the exact Bahcall-Schmidt-Soneira potential.

tunga and Freeman (1985, hereafter RF). In addition, we consider only shell orbit models, already discussed in § II. They are attractive for their simplicity, both conceptually and analytically.

We simplify equations (6) and (8) even further by assuming that the mass density can be factorized: $\rho(\lambda, v) = \rho_\lambda(\lambda)\rho_v(v)$. This has the advantage that then none of the kinematical quantities depends on ρ_λ , just as is the case for a component built with spherical orbits only. The confocal spheroids of constant λ rapidly become nearly spherical as λ increases, and therefore $\rho_v(v)$ is related to the flattening of the component. For simplicity, we also ignore any v -dependence. The kinematical quantities now depend only on the potential, through the R -function. These simplifications imply that the shell orbit component is almost spherical. According to the studies of White (1985) and Sommer-Larsen (1987) this should give an adequate representation of the data.

For construction of a more realistic model one can choose ρ_v such that it corresponds to a population that is somewhat concentrated toward the Galactic plane, and redo the calculations of the kinematical properties. However, in this case it is probably better to lift the requirement that $\rho(\lambda, v)$ factors.

Figure 4 shows the RF data in their SA 141 field, at $l = 240$ and $b = -85$. The data indicate a line-of-sight velocity dispersion of the order of 60 km s^{-1} at a position of 15–20 kpc above the plane, with a rather substantial uncertainty of a few tens of km s^{-1} , probably due to the small number statistics. As pointed out in the above, if the distribution of K giants at that altitude were isotropic, we would expect a dispersion of the order of $V_c/3^{1/2} \approx 120 \text{ km s}^{-1}$, with V_c the local circular velocity. The dashed curve is the mean line-of-sight velocity v_{los} as

calculated for the shell model, assuming that all stars move in the direction of Galactic rotation. The outer curves are $\langle v_\phi \rangle \pm \sigma_{\text{los}}$, for the case of no net rotation (*thick curves*) and for the case of maximum streaming (*thin curves*). They are only drawn for locations with $|z| \geq 5 \text{ kpc}$, since we do not expect shell orbit models to be valid in regions of low galactic altitude. Clearly the data are compatible with a model in which the stars are moving on shell orbits. The small observed dispersion is due to the fact that the line-of-sight is almost aligned with the λ -direction, which has no dispersion in this case. This result is not surprising, since Sommer-Larsen (1987) was able to reproduce the observed velocity dispersion in this field with stars on circular orbits in a simple spherical potential.

Figure 5 shows the SA 127 field surveyed by RF, at $l = 270$ and $b = 38$. The thick curves again show $\langle v_\phi \rangle \pm \sigma_{\text{los}}$ for the case of no net rotation. Here the agreement between the observed velocities and the shell model is clearly less satisfactory than in the high-altitude field of Figure 4. The σ_{los} predicted by the model is much smaller than is observed. This is to be expected, since a λ component must be present at lower galactic altitudes, and it is not taken into account. It may indicate that the K giant component is flattened, since then the radial component becomes more important towards the disk. This is in agreement with the analysis of White (1985) and Levison and Richstone (1986).

We have seen in § IIc that shell orbits can be considered as slowly precessing elliptic orbits. From equation (5) it follows that at a galactocentric radius of 15 kpc the precession period of the orbital plane, and hence the time scale for the spreading of stars within the shell, is of the order of $3 \times 10^9 \text{ yr}$, which is about 8 times larger than the orbital period at this radius. At

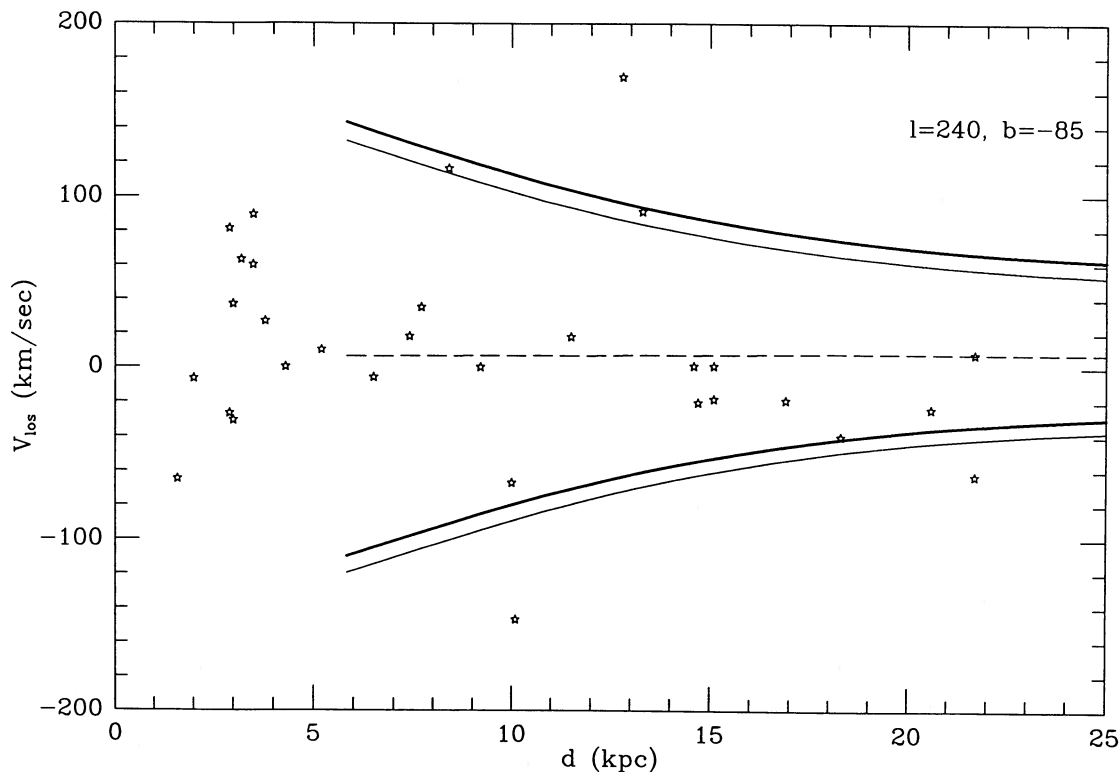


FIG. 4.—Data for RF's SA 141 field. Abscissa is distance from the Sun; ordinate is the line-of-sight velocity dispersion. The dashed curve is the mean velocity, assuming maximum streaming in the direction of Galactic rotation. The thin curves show the 1σ variations in the case of maximum streaming. The thick curves are analogous, but for no net streaming.

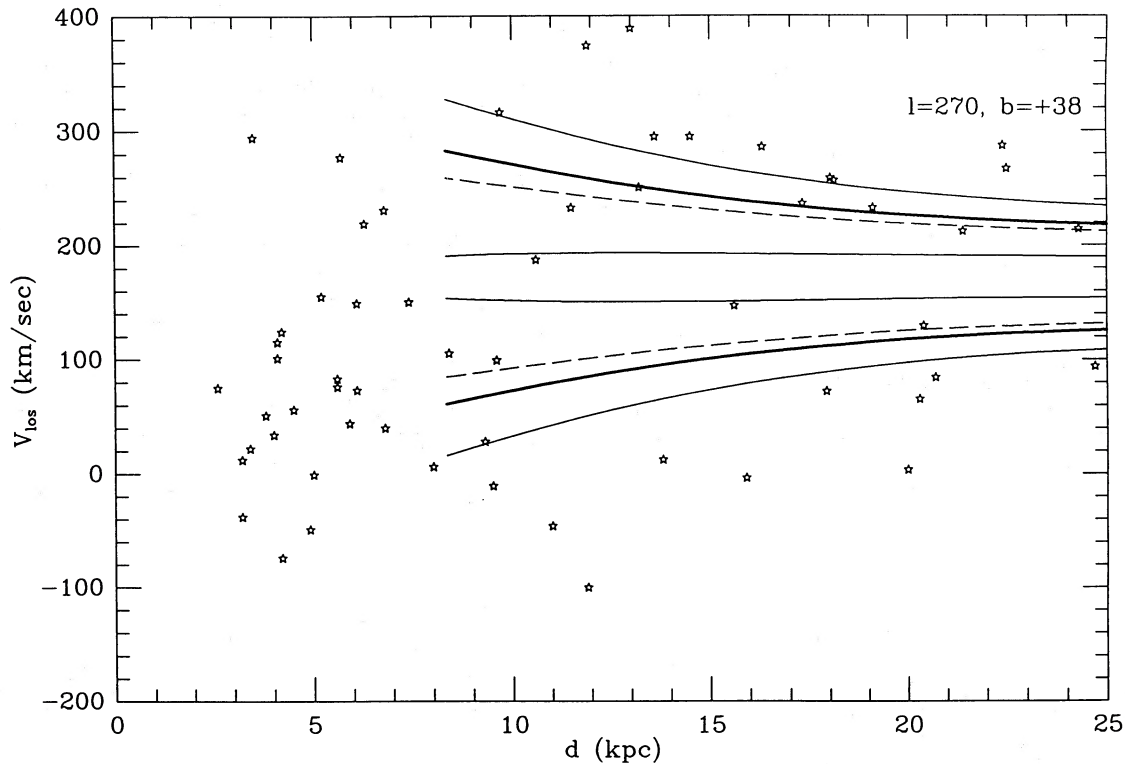


FIG. 5.—Same as Fig. 4, but for RF's SA 127 field. The thick curves show $\langle v_\phi \rangle \pm \sigma_{\text{los}}$ for the case of no net rotation. The dashed curves give the mean streaming for retrograde (*upper*) and direct (*lower*) motion with respect to Galactic rotation. The thin curves give the 1σ variations.

5 kpc the precession period is of the order of 4×10^8 years (three times the orbital period).

Statler (1988) has shown that dynamical friction on a small companion galaxy tends to deposit stars preferentially on thin tube orbits. If indeed repeated infall has caused the presence of K giants at high galactic altitude, then the precession times indicate that these stars should be seen in clumps. In this respect, it is interesting to note that the distribution of velocities in Figure 5 shows a tendency to be bimodal at large z . The lower dashed curve gives the mean streaming velocity for stars on shell orbits that all move in the direction of Galactic rotation, and the lower thin curves show the 1σ dispersion. The upper curves are similar, but for retrograde stars exclusively. This gives a somewhat better representation of the data than does the model with equal numbers of stars going in both directions. We remark that clumpiness in the halo population has been suspected by other authors as well (Norris 1986; Freeman 1987).

V. CONCLUDING REMARKS

The main result of this study is that the Galactic potential can be represented fairly accurately by a potential that is of Stäckel form. This implies that many, although by no means all, properties of the stellar orbits in the Galaxy can be derived by a study of the best-fitting Stäckel model. Since three exact integrals of motion are known for a Stäckel potential, the dynamics is accessible by analytic means, and models with truly anisotropic velocity distributions can be constructed. Furthermore, since the potential is described by a function of one variable only, many of the required calculations can be done in an efficient and transparent way.

We have obtained a global fit to the Bahcall-Schmidt-Soneira potential with an error not worse than 3%. If one is interested in the potential in a smaller region, e.g., near the disk, then a local fit can be made with even higher accuracy. The fit is least satisfactory in the central regions and should not be used there, especially since the Galactic bulge may well be nonaxisymmetric.

As a simple example, we have discussed the dynamics of the Population II stars at high Galactic altitude. Use of the special shell orbits allowed us to derive kinematic properties in a straightforward manner. The available data are consistent with the K giants at high Galactic altitude being predominantly on tube orbits that have small radial excursions.

The analysis presented in § IV can be extended easily to include more realistic density components. DZ show that a variety of simple choices for the distribution function $F(E, I_2, I_3)$ give rise to smooth density components for which the corresponding velocity dispersions can be given explicitly also. Presumably, such components can be used to fit the kinematics of other Galactic populations with a known density distribution as well. Candidates are the various halo samples that have been obtained recently (e.g., Norris 1986; Sandage 1987; Gilmore and Wyse 1987), and also the OH/IR stars in the bulge and the disk, for which radial velocities are now being measured (Habing 1987).

In some cases it may be more convenient to use the equations of stellar hydrodynamics in order to derive velocity dispersions directly from the density distribution. For axisymmetric Stäckel models, the general solution of these equations is available (see DZ). The disadvantage of this approach is that additional information is needed to specify

the dispersions uniquely. Also, it is not always guaranteed that the resulting dispersions correspond to a physical, i.e., non-negative, distribution function.

We note that, although the magnitude of the velocity dispersions must be calculated by one of the methods just indicated, the orientation of the velocity ellipsoid is known. As already mentioned in § II*d*, Eddington (1915) showed that in a Stäckel model the principal axes of the velocity ellipsoid are everywhere aligned with the coordinates in which the equations of motion separate. The fact that a Stäckel model can be fitted to the Galactic potential therefore suggests that in a first approximation the principal axes of the velocity ellipsoids of Galactic populations are aligned with the corresponding prolate spheroidal coordinates. In the halo these coordinates are very closely approximated by spherical coordinates, so that here one principal axis points radially, another one points tangentially to the pole, and the third lies in the rotation direction. The latter may also be the direction of the major axis of the velocity ellipsoid.

The distribution of mass in our Galaxy is fairly well known, and accurate starcount models have been constructed (Bahcall 1986). Inclusion of kinematic data in the models is the obvious next step. The results presented here indicate that this can be done in an efficient and physically consistent way by use of a Stäckel potential that fits the Galactic potential. Such a model for the Galaxy may well be adequate for a number of purposes and should be a good guide for the interpretation of kinematic observations and for the construction of more detailed numerical models.

It is a pleasure to thank Martin Schwarzschild and John Bahcall for enlightening conversations and a critical reading of the manuscript. Luis Aguilar kindly made available various programs for the calculation of the Galactic potential. This research was supported in part by NSF grant PHY8620266, and by an RCA Fellowship to T. dZ.

REFERENCES

- Bahcall, J. N. 1986, *Ann. Rev. Astr. Ap.*, **24**, 577.
 Bahcall, J. N., and Soneira, R. M. 1980, *Ap. J. Suppl.*, **44**, 73.
 Bahcall, J. N., Schmidt, M., and Soneira, R. M. 1982, *Ap. J. (Letters)*, **258**, L23.
 Bishop, J. 1987, *Ap. J.*, **322**, 418.
 Caldwell, J. A. R., and Ostriker, J. P. 1981, *Ap. J.*, **251**, 61.
 Dejonghe, H., and de Zeeuw, P. T. 1988, *Ap. J.*, submitted (DZ).
 de Zeeuw, P. T. 1984, Ph.D. thesis, Leiden University.
 ———. 1985, *M.N.R.A.S.*, **216**, 273 (Paper I).
 ———. 1988, in preparation (Paper II).
 de Zeeuw, P. T., and Lynden-Bell, D. 1985, *M.N.R.A.S.*, **215**, 713.
 de Zeeuw, P. T., Peletier, R. F., and Franx, M. 1986, *M.N.R.A.S.*, **221**, 1001.
 Eddington, A. S. 1915, *M.N.R.A.S.*, **76**, 37.
 Freeman, K. C. 1987, *Ann. Rev. Astr. Ap.*, **25**, 603.
 Gilmore, G., and Wyse, R. F. G. 1987, in *The Galaxy*, ed. G. Gilmore and R. F. Carswell (Dordrecht: Reidel), p. 247.
 Habing, H. J. 1987, in *The Galaxy*, ed. G. Gilmore and R. F. Carswell (Dordrecht: Reidel), p. 173.
 Hori, G. 1962, *Pub. Astr. Soc. Japan*, **14**, 353.
 Kuzmin, G. G. 1956, *Astr. Zh.*, **33**, 27.
 Levison, H. F., and Richstone, D. O. 1986, *Ap. J.*, **308**, 627.
 Martinet, L., and Mayer, F. 1975, *Astr. Ap.*, **44**, 45.
 Morse, P. M., and Feshbach, H. 1953, *Methods of Theoretical Physics* (New York: McGraw-Hill), chap. 5.
 Norris, J. E. 1986, *Ap. J. Suppl.*, **61**, 667.
 Ollongren, A. 1962, *Bull. Astr. Inst. Netherlands*, **16**, 241.
 Oort, J. H. 1965, in *Stars and Stellar Systems*, Vol. 5, *Galactic Structure*, ed. A. Blaauw and M. Schmidt (Chicago: University of Chicago Press), p. 455.
 Pier, J. R. 1982, *A.J.*, **87**, 1515.
 ———. 1983, *Ap. J. Suppl.*, **53**, 719.
 Ratnatunga, K. U., and Freeman, K. C. 1985, *Ap. J.*, **291**, 260.
 Richstone, D. O., and Tremaine, S. D. 1984, *Ap. J.*, **286**, 27.
 Sandage, A. R. 1987, in *The Galaxy*, ed. G. Gilmore and R. F. Carswell (Dordrecht: Reidel), p. 321.
 Schmidt, M. 1956, *Bull. Astr. Inst. Netherlands*, **13**, 15.
 Schwarzschild, M. 1979, *Ap. J.*, **232**, 236.
 Sommer-Larsen, J. 1987, *M.N.R.A.S.*, **227**, 21P.
 Sommer-Larsen, J., and Christensen, P. R. 1986, *M.N.R.A.S.*, **219**, 539.
 Stäckel, P. 1890, *Math. Ann.*, **35**, 91.
 Statler, T. S. 1988, *Ap. J.*, in press.
 van de Hulst, H. C. 1962, *Bull. Astr. Inst. Netherlands*, **16**, 235.
 Wayman, P. A. 1959, *M.N.R.A.S.*, **119**, 34.
 White, S. D. M. 1985, *Ap. J. (Letters)*, **294**, L99.

HERWIG DEJONGHE AND TIM DE ZEEUW: Institute for Advanced Study, Princeton, NJ 08540